Measurement of the Water Droplet Size in Water-in-Oil Emulsions Using Low Field Nuclear Magnetic Resonance for Gas Hydrate Slurry Application

ARTICLE *in* CANADIAN JOURNAL OF CHEMISTRY · APRIL 2015

Impact Factor: 1.06 · DOI: 10.1139/cjc-2014-0608

4 AUTHORS, INCLUDING:

Milad Saidian

21 PUBLICATIONS **15** CITATIONS

SEE PROFILE

Manika Prasad

Colorado School of Mines

114 PUBLICATIONS **859** CITATIONS

SEE PROFILE

Carolyn Ann Koh

Colorado School of Mines

186 PUBLICATIONS **4,522** CITATIONS

SEE PROFILE

Rapid #: -9327503

CROSS REF ID: **42080**

LENDER: **NED :: Snell Library**

BORROWER: **COP :: ArthurLakesLibrary**

TYPE:	Article CC:CCG
JOURNAL TITLE:	Canadian journal of chemistry
USER JOURNAL TITLE:	Canadian Journal of Chemistry
ARTICLE TITLE:	Measurement of the Water Droplet Size in Water-in-Oil Emulsions Using Low Field Nuclear Magnetic Resonance for Gas Hydrate Slurry Application
ARTICLE AUTHOR:	Ahmad Afif Majid, Milad Saidian, Manika Prasad, Ca
VOLUME:	
ISSUE:	
MONTH:	15 April
YEAR:	2015
PAGES:	e-pub
ISSN:	0008-4042
OCLC #:	

Processed by RapidX: 5/26/2015 12:41:52 PM

Measurement of the Water Droplet Size in Water-in-Oil Emulsions Using Low Field Nuclear Magnetic Resonance for Gas Hydrate Slurry Application

Ahmad AA Majid[1], Milad Saidian[2], Manika Prasad[2], Carolyn A. Koh[1*]

1. Center for Hydrate Research, Department of Chemical and Biological Engineering, Colorado School of Mines, 80401 USA
2. Department of Petroleum Engineering, Colorado School of Mines, 80401 USA

Abstract

Turbulent flow in the oil and gas pipelines often results in the formation of a water-in-oil (W/O) emulsion. Small water droplets in the pipeline provide large total surface area for hydrate formation at the water/gas saturated oil interface, which can lead to full conversion of water to gas hydrate. As a result, this may prevent the formation of large hydrate aggregates that can cause hydrate particle settling and eventually plugging. It is thus of particular interest to determine the water droplet size of an emulsion. Since water droplet size of the emulsion provides information about the hydrate particle size in the slurry, it is crucial to determine the water droplet size in a W/O emulsion. In this work, the water droplet size of model W/O emulsion systems were measured using two techniques: Diffusion-Transverse Relaxation (T_2) experiments using low field Nuclear Magnetic Resonance (NMR) and optical microscopy image analysis techniques. The T_2 distribution of the emulsion was also measured. The water volume fraction was varied from 10 – 70 vol.%. The NMR and microscopy image analysis results show the droplet size ranging from 3.5 to 4.5 μm and 2 to 3 μm, respectively. Both techniques show a minimum 2 and 4 μm at 50 vol.% water cut. There are two main reasons for the small difference in droplet size distribution (DSD) measured using these techniques: NMR provides DSD of the entire emulsion sample as opposed to an optical microscopy

technique that only capture a small sample of the emulsion. In addition, since the NMR method does not require sample preparation, the characteristics and properties of the emulsion are maintained. On the contrary, using microscopy images, the sample is compressed between two glass slides. This will disturb the properties of the emulsion. By combining the diffusion-T_2 and T_2 distributions, the surface relaxivity was determined to be 0.801 μm/s for the oil/water emulsion. The DSD obtained from the NMR method in this work was compared with microscopy analysis, and results show there is reasonable agreement between the two methods. This paper provides a comparison of the two methods that can be used to determine the water droplet size of W/O emulsions. This study indicates that a relatively simple quantitative NMR method can be utilized to determine the water droplet size of W/O emulsions before gas hydrate formation, and hence can be used to assess the gas hydrate slurry properties and plugging risk of W/O systems.

Keywords: emulsion, plugging, droplet size, diffusion, surface relaxavity

Introduction

Gas hydrates (also known as clathrate hydrates) are crystalline compounds in which small gas molecules such as methane, ethane, propane and cyclopentane are enclathrated by hydrogen-bonded water molecules (1). The water molecules form a network of hydrogen bonds around the gas molecules thereby forming water cages. Gas hydrates typically form at high pressure and low temperature (e.g. 10 MPa, 277 K for methane hydrates) (1). At these conditions, hydrates can form and plug subsea oil/gas pipelines and are considered a nuisance.

Figure 1 shows a conceptual schematic of hydrate formation in pipelines for an oil-dominated system (i.e. where oil is the continuous phase). Hydrate formation begins with water being emulsified in the oil phase forming a water-in-oil (W/O) emulsion. As explained below, this emulsion may or may not be desirable depending on the size of the water droplets. Next, at appropriate pressure and temperature condition, a thin hydrate shell will grow around the water droplets (1). If the water droplet is in the μm size range, gas molecules are able to penetrate through the shell. In this case, hydrates will grow

inward forming fully converted hydrate particles that can prevent hydrate agglomeration and pipeline blockage. However, this hydrate shells can create a gas diffusion barrier between the oil and the water phase if water droplets are bigger than μm size range (1). Then there will be capillary attraction forces between hydrate particles due to water bridging (from unconverted free water) that cause the particles to agglomerate forming large hydrate aggregates (1). Since these aggregates may then form a blockage in the pipeline, it is crucial to determine the water droplet size in an emulsion and eventually the hydrate particle size in a slurry.

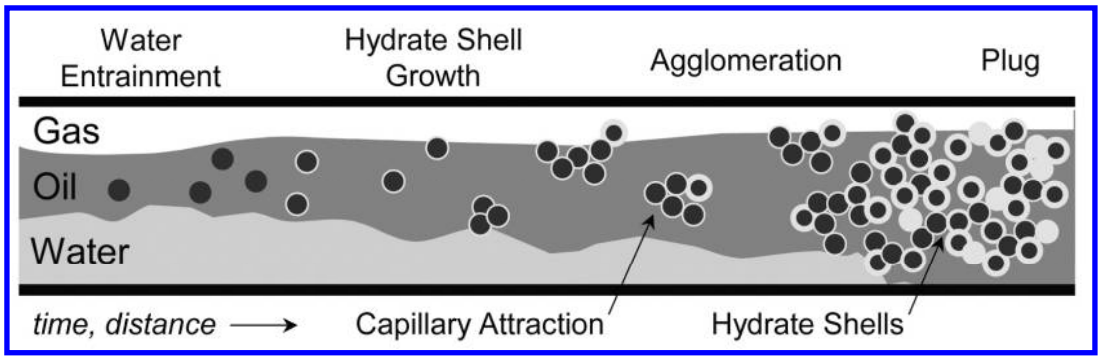

Figure 1: Conceptual schematic of hydrate plug formation in pipeline for oil dominated system (redrawn from (2) and J. Abrahamson, (3)).

There are several methods being employed by researchers and operators to determine droplet size of the emulsion such as microscopy (4), and Nuclear magnetic resonance (NMR) (5–7). Each method has its own advantages and disadvantages. For instance, the microscopy imaging method is relatively simple and fast. The size of the droplet is measured by analyzing optical microscopy images of the emulsion. However, in this method, only a small sample of the emulsion is analyzed (e.g. ~250 water droplets) and thus the method may not reflect the actual condition in pipelines. Another method to determine the DSD of emulsions is using NMR. This method has gained interest since it is non-destructive and can measure a considerable amount of sample.

In this paper, the DSD of the system is determined by studying the diffusion of the system using NMR, specifically by taking advantage of the differences in relaxation times for oil and water. In this work, we present a method for the conversion of the T2 distribution signal to droplet size distribution.

Materials and Methods

Emulsion Preparation

The model water-in-oil emulsion consists of a mineral oil, a mixture of surfactants and deionized water. The mineral oil in this work was Crystal Plus mineral oil 70T purchased from STE Oil Company Inc. The oil is a Newtonian fluid with a viscosity of 20 cP at 25 °C and density of 0.857 g/cm^3 at 20 °C. The chemical composition of the mineral oil is given in Table S1.

The surfactant mixture consists of a nonionic surfactant, Sorbitan Monooleate (known as Span 80) and an ionic surfactant, Sodium Di-2-Ethylhexylsulfosuccinate (known as AOT). The molecular structures of the surfactants are shown in Figure 2. The concentration of surfactant in the model W/O emulsions is 5 wt.% with respect to the total mass of the emulsion. Furthermore, the ratio concentration of the surfactants used in this work is 90 wt.% of Span 80 and 10 wt.% of the AOT. Span 80 was purchased from Sigma Aldrich. It has a reported molecular weight of 428.61 g/mol and Hydrophilic Lipophilic Balance (HLB) value of 4.3 (8). AOT surfactant was purchased from Fischer Scientific and has a reported molecular weight of 444.56 g/mol. The water volume fraction (also known as water cut) for this model emulsion system ranges from 10 to 70 vol.%.

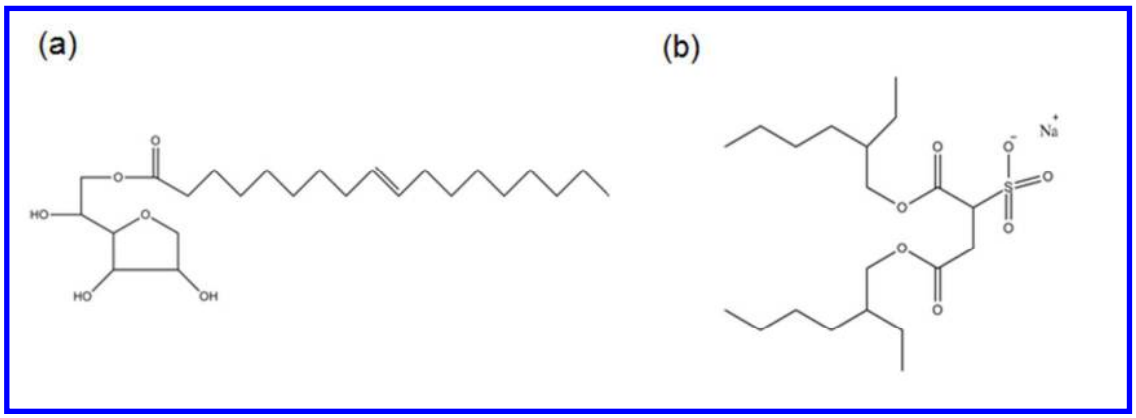

Figure 2: Molecular structure of the surfactants used in this work, (a) Span 80 and (b) AOT.

In this work, 30 ml of emulsion sample was prepared by first, dissolving the pre-weighed surfactant mixture in the mineral oil at low heat (~50°C) and medium stirring. This was done using a hotplate and a magnetic stirrer. Next, the sample was cooled to room temperature. Once cooled, the sample was stirred at 8000 rpm using a high-speed

homogenizer (Virtis Sentry Cyclone IQ2 Homogenizer), while water was added slowly using a syringe. (9). The total stirring time depends on water cut of the emulsion. For emulsions with water cuts ≤ 50 vol. %, the system was stirred for 3 minutes where water was added during the first minute. As for 60 and 70 vol.% water cut emulsions, the system was stirred for 6 minutes and water was added during the first 4 minutes. A longer stirring time was required for the high water cut system to allow water to be added slowly into the system. This method ensures that W/O emulsion will be produced.

Microscopy Droplet Size Measurement

The water droplet size of the emulsion was measured using an optical microscope (Olympus IX71) connected to a digital camera (Olympus XM10). The microscope images were analyzed using ImageJ. At each water cut investigated, a minimum of 250 water droplets were measured and the mean droplet size was calculated and reported in this work.

NMR Droplet Size Measurements

The NMR measurements were performed using a 2 MHz Magritek Rock Core Analyzer. All measurements are at room temperature and pressure. Two main pulse sequences are used to measure the NMR response for the emulsion samples. In this section, the pulse sequences and the analysis techniques are discussed.

Carr-Purcell-Meiboom-Gill (CPMG) Pulse Sequence

The CPMG pulse sequence (Figure 3) was introduced by Carr and Purcell (1954) and then modified by Meiboom and Gill (1958) to measure the transverse relaxation time (T_2) of hydrogen nuclei in fluid samples. The T_2 relaxation mechanism is a combination of three relaxation mechanisms (Equation 1): bulk relaxation (T_{2B}), surface relaxation (T_{2S}), and diffusion induced relaxation (T_{2B}) (10).

$$\frac{1}{T_2} = \frac{1}{T_{2B}} + \frac{1}{T_{2S}} + \frac{1}{T_{2D}} \qquad \textbf{Equation 1}$$

By minimizing the echo spacing (TE in Figure 3) the diffusion induced relaxation becomes negligible compared to bulk and surface relaxations (11). Surface relaxation is a function of surface relaxivity and the ratio of surface area to the volume. Assuming spherical-shaped droplets for the discontinuous phase (water in this study), Equation 1 can be rewritten as (Equation 2):

$$\frac{1}{T_2} = \frac{1}{T_{2B}} + \rho\frac{S}{V} = \frac{1}{T_{2B}} + \rho\frac{3}{r} \qquad \textbf{Equation 2}$$

In which ρ is the surface relaxivity, S is the surface area, V is the volume, r is the droplet radius. This equation can be solved for droplet radius, which is the main focus of this study (5):

$$r = 3\rho\left(\frac{1}{T_2} - \frac{1}{T_{2B}}\right)^{-1} \qquad \textbf{Equation 3}$$

Bulk and T_2 distributions in Equation 3 can be measured for the emulsion, the only parameter that is required for droplet size calculation is the surface relaxivity.

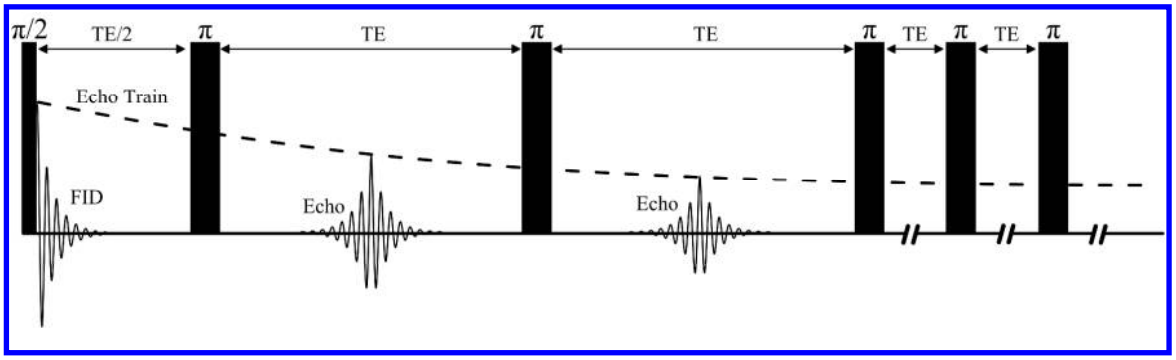

Figure 3: Schematic of the CPMG pulse sequence (5). This pulse sequence is the most common sequence used to measure the T_2 distribution (5). FID is the free induction decay, π and π/2 are the 180 and 90 degrees pulses, TE is the echo spacing which is the time between two consecutive 180 degrees pulses. Echo train (the dashed line) is the raw data for T_2 distribution measurement.

All the NMR measurements were performed using a 2 MHZ Magritek Rock Core Analyzer at room temperature and pressure. The T_2 distributions were measured with 400

µs echo spacing, 50000 number of echoes, constant pulse length of 20µs for both 90 and 180 degrees pulses and minimum signal to noise ratio (SNR) of 250.

Pulsed Field Gradient-CPMG Pulse Sequence

The Pulsed Field Gradient-CPMG pulse sequence consists of a pulse field gradient (PFG) followed by a CPMG pulse sequence. This pulse sequence correlates two phenomena: the translational diffusion coefficient of water molecules restricted by droplet walls (replicated in the diffusion measurement) and the chemical properties of water and oil (replicated in the T_2 measurement). A two dimensional distribution function accounts for these phenomena and an inverse Laplace transform is used to produce the D-T_2 maps. We used non-negative least square (NNLS) algorithm for 2d inversion of D-T_2 data (12). More information about D-T_2 data acquisition and mathematical inversion can be found in (13–15). The smoothing parameter for the inversion has been chosen by the method described by (16).

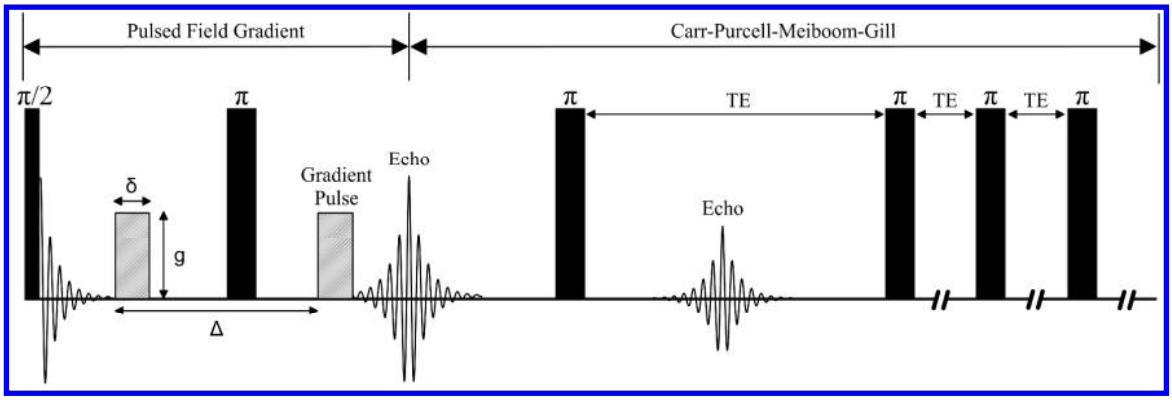

Figure 4: Schematic of the PFG-CPMG pulse sequence (modified from 5). This pulse sequence consists of a pulsed field gradient pulse sequence followed by a CPMG pulse sequence. It is used to measure the D-T_2 maps. π and π/2 are the 180 and 90 degrees pulses, Δ is the diffusion time which is the time between gradient pulses, $\boldsymbol{\delta}$ is the gradient pulse duration, TE is the echo spacing which is the time between two consecutive 180 degrees pulses.

Discontinuous phase diffusion coefficient can be measured using only PFG pulse sequence (6,17–19). PFG pulse sequence measures the diffusion coefficient of a combination of both continuous and discontinuous phases. There are two methods to measure the discontinuous diffusion coefficient: In the first approach differentiating the diffusion coefficient requires knowledge of the fraction of the continuous phase (6,17–

20) which is usually unknown in cases such as oil and gas production wells and pipelines. The second approach is to use very long diffusion times to allow the continuous phase NMR signal to decay during this time period (7,18,19,21,22). The disadvantages of this approach are compromising the signal to noise ratio since a major portion of the signal decays due to relaxation before the data acquisition and also applicability only in cases that the continuous phase relaxation is faster than the discontinuous phase.

In this study we used 2D D-T_2 maps, even though the experiment time is longer than PFG experiments. Using 2D maps we can differentiate the water and oil diffusion responses based on their respective T_2 distributions. The 2D maps were measured using 30 ms diffusion time, 5 ms gradient pulse duration, 0.5 T/m maximum gradient and 40 gradient steps. The CPMG part of the pulse sequence is ran using the CPMG pulse sequence for 1d T_2 experiments. Figure 5 shows an example of the 2D map specifically the 20% water cut emulsion.

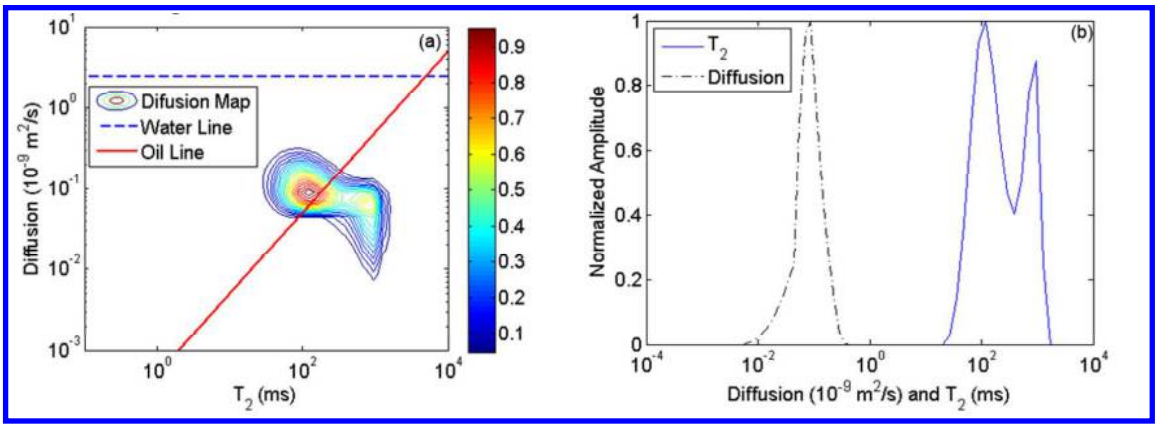

Figure 5: (a) 2D D-T_2 map for 20 vol.% water cut emulsion and (b) corresponding Diffusion coefficient and T_2 distribution extracted from 2D map. In (a) Both water and oil responses are shown distinctively, but separate D and T_2 responses were not able to resolve the differences. The water line is the diffusion coefficient measured for bulk water used in this study and the oil line is calculated based on the correlation by Lo et al. (2002) (23)

The diffusion values are converted to radius using the following approach. The water molecules are restricted by the droplet walls; as a result the measured diffusion is lower than the bulk water diffusion. This reduction in diffusion coefficient value depends on the droplet size and the PFG acquisition parameters. Murday and Cotts (1968) developed a model to relate the echo-signal attenuation to the diffusion coefficient of the fluid in a

sphere with specific radius considering the experimental acquisition parameters (24). We use this model to calculate the droplet radius using measured diffusion coefficients.

Results and Discussions

Microscopy Droplet Size Measurements

Figure 6 shows the microscopy images of the water-in-oil emulsions prepared using mineral oil 70T at 10 and 50 vol.% of water cut. Analysis of the microscopy images shows that the numerical average droplet size of this emulsion system is in the range of 2 – 3 μm across all water cut emulsions investigated in this work (Figure 7). It is to be mentioned here that at each water cut a minimum of 250 water droplets were measured. From these measurements, the average droplet size and its standard deviation was calculated. The error bar in Figure 7 represents the standard deviation in the measurements. This average droplet size is in agreement with a typical water-in-crude oil emulsion system reported by us and other researchers (25).

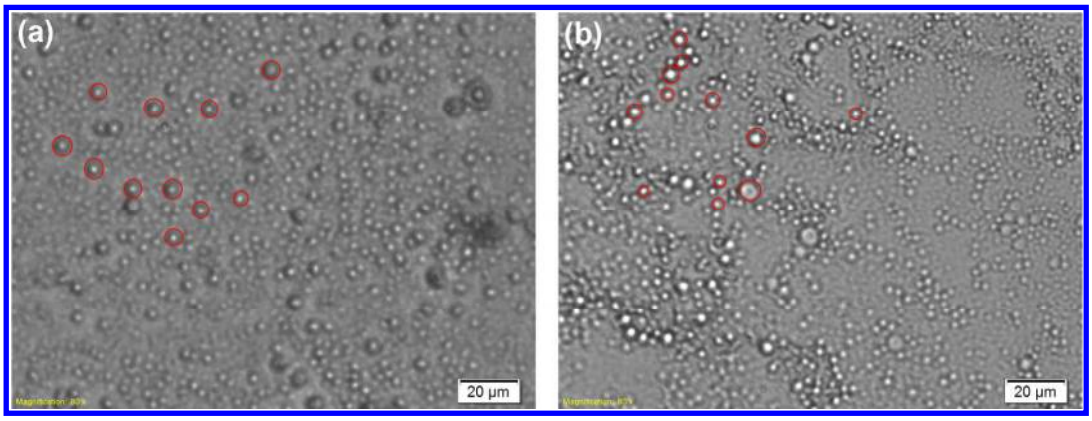

Figure 6: Microscopy images of mineral oil 70T emulsion system at (a) 10 vol.% and (b) 50 vol.% water cut. Red lines indicate the boundary.

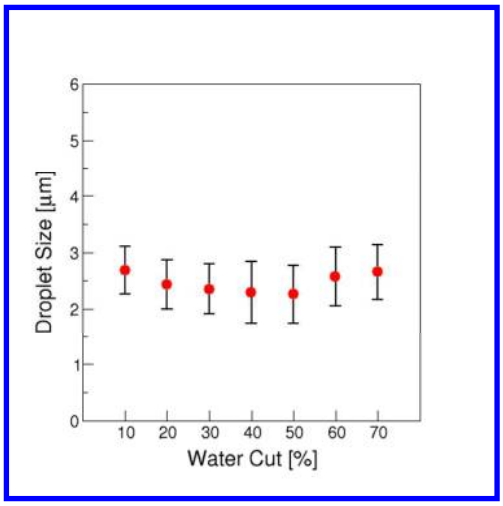

Figure 7: Microscopy droplet size measurement for mineral oil 70T emulsions at various water cuts (vol.%).

The microscopy water droplets size measurement shows that there is minimal change in the size of the water droplets across the water cuts investigated in this work. It is likely that the water droplet size does not change due to the high concentration of surfactant used in this work (22). Our study shows that the critical concentration of aggregation (CCA), which is, the concentration at which inverse micelles form was measured to be 0.1 wt.% for all water cuts (4). Thus, the emulsions used in this work were prepared at concentrations above the CCA.

NMR Droplet Size Measurements

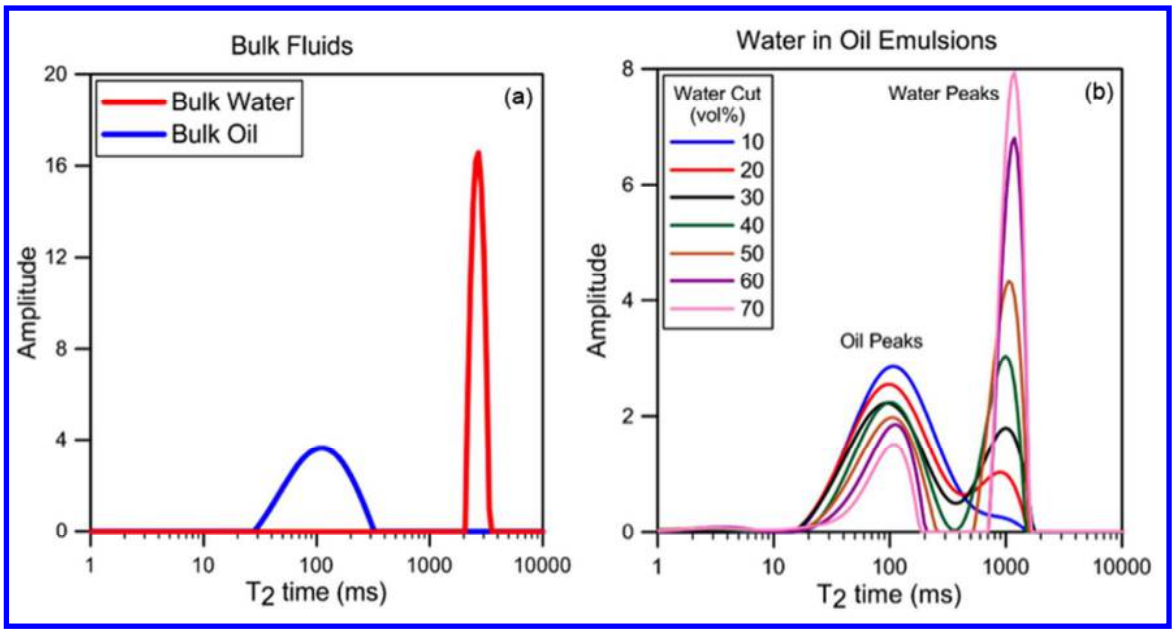

Figure 8: T_2 distirbution for (a) bulk oil and water and (b) emulsions at various water cuts

Figure 8 shows the T_2 distribution for bulk oil and water as well as all the emulsions measured using the CPMG pulse sequence (Figure 3). Bulk responses show a clear distinction between oil and water T_2 distributions (**Figure 8**(a)). When water is emulsified in the oil phase, the T_2 response for the discontinuous phase (water droplet) is affected by the emulsion properties. **Figure 8**(b) shows the T_2 response for emulsion samples. The T_2 relaxation times for oil do not change by varying the water cut because oil is the continuous phase. T_2 response for water varies depending on the water cut. The surface relaxivity for the emulsions can be calculated by solving Equation 3 for ρ. We used the T_2 distribution of the water phase for samples with water cut of 50-70 vol% since they show a distinct peak for water phase. The average surface relaxivity is 0.801 μm/s (6,18). By having this surface relaxavity value, droplet size of any T_2 distribution for this mineral oil and water system can be calculated using Equation 3. Using this calculated surface relaxivity, the droplet size derived from T_2 distributions and Equation 3, varies from 3.3 to 4.7 μm which is close to the range of the droplet size measured by diffusion method. The difference is because for low water cut samples (10 to 30 vol%) samples the water T_2 distribution is not distinct from the oil distribution.

Figure 9 shows the numerical average water droplet size across all water cut emulsions studied in this work determined from NMR investigations. As can be seen in Figure 9, the average droplet size is ~ 4 μm. In this figure, the error bar represents the smallest and largest water droplets detected in these measurements from T2 data. Similarly to the microscopy analysis, the size of water droplets shows minimal change with change in the water cut of the system. As mentioned earlier, the relatively constant water droplet size across the water cuts is likely to be due to the high concentration of surfactant used in this study. However, it should be mentioned here that the minimum water droplet size observed at 50 vol.% water cut is relatively small and thus not significant.

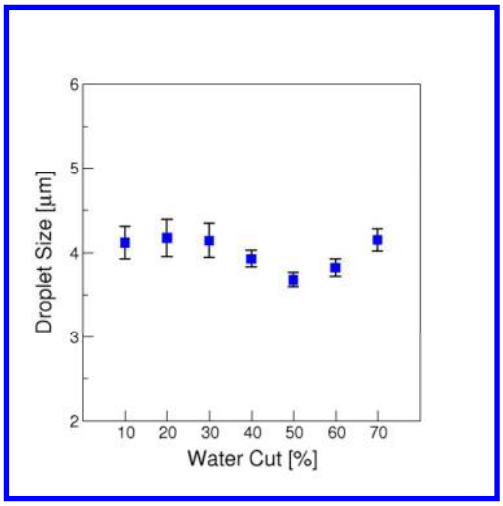

Figure 9: NMR droplet size measurements for mineral oil 70T emulsions at various water cuts.

Comparison between NMR and Microscopy Results

Figure 10 shows the comparison of the water droplet size obtained from the two methods used in this work: NMR and optical microscopy measurements. From Figure 10, the size of the water droplet reported in both methods is in the same order of magnitude, with the NMR method showing a slightly larger droplet size (average of 1 µm larger) as compared to the optical microscopy method. The difference in the size of the water droplet reported by both methods is currently being investigated. Some of the expected error from optical microscopy method includes poor edge detection due to the shadow effects.

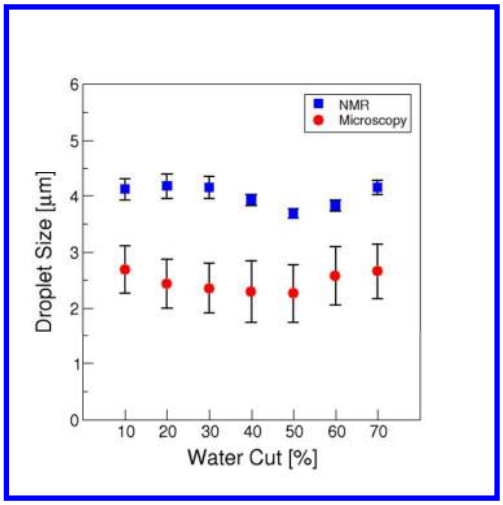

Figure 10: Comparison of NMR and Microscopy water droplet size for all water cuts (vol. %).

Furthermore, it can be seen in Figure 10 that in both methods, the trend of the water droplets across all water cuts studied is relatively similar; both show a minimum

droplet size at 50 vol.% water cut. This shows that the NMR method proposed here is able to measure the water droplet size in emulsion systems. In addition, it should be noted that when comparing the two methods, larger deviation was observed for the microscopy method results as compared to the NMR method. It is thought that this large deviation in the size of the water droplet measured is due to the optical microscopy method that was used. In optical microscopy, actual position of the droplets in the z-axis (vertically) could not be determined. Consequently, the droplets that are far from the lens appear smaller in the pictures taken. The size of the droplets was measured regardless of the vertical position of the droplets size and the result was taken into the calculation of the average droplet size. This resulted to a smaller average droplet size.

Conclusions

Our results have shown that Diffusion-Transverse Relaxation (T_2) experiments using a low field NMR method can be used to measure the DSD of an emulsion sample. The results obtained from this method were compared with the results obtained from microscopy image analysis techniques. The investigations show that the average droplet size obtained from NMR is on average 1 μm larger as compared to the microscopy technique. However, both methods show a similar trend across the water cuts investigated in this work. There are relatively small changes in the size of the water droplets across the water cuts studied here. The method also allows the determination of average surface relaxivity for water droplets in an oil continuous phase and was calculated to be 0.801 μm/s. The determination of average surface relaxivity of this model emulsion system, allows direct calculation and determination of average water droplet size in this model system without performing diffusion test. This NMR method will be immensely useful in determining the droplet size of water-in-oil emulsions, and hence provides a simple quantitative approach to assessing gas hydrate slurry formation and hydrate plugging risk.

Acknowledgement

The authors would like to thank Sophie Godeferoy, Brett Ryland and Paul T. Callaghan from Victoria University of Wellington for providing the inverse Laplace transform program for 2D inversions. The authors would also like to thank Dr. John Ripmeester and Evan McCarney for all the valuable discussion and input that he has provided on this work. Additionally, Ahmad AA Majid would like to thank Universiti Malaysia Pahang and Malaysian Ministry of Education for sponsoring his studies.

References

1. Sloan, E.D.; Koh C.A. *Clathrate Hydrates of Natural Gases,* CRC Press, **2007**.

2. Turner, D.J. *Colorado School of Mines*, **2006**.

3. Turner, D.J; Miller, K.T; Sloan, E.D. *Chem. Eng. Sci.* **2009**, 64 (18), 3996. doi: 10.1016/j.ces.2009.05.051

4. Delgado-Linares J.G; A. Majid, A.A; Sloan, E.D; C. Koh, C.A; Sum, A.K. *Energy & Fuels*. **2013**, 27 (8), 4564. doi: 10.1021/ef4004768.

5. Aichele, C.P.; Flaum, M.; Jiang, T; Hirasaki, G.J.; Chapman, W.G. *J. Colloid Interface Sci.* **2007**,315 (2), 607. doi:10.1016/j.jcis.2007.07.057.

6. Fridjonsson, E.O.; Flux, L.S.; Johns, M.L. *J. Magn. Reson.* **2012**, 221, 97. doi:10.1016/j.jmr.2012.05.012.

7. Opedal, N.V.D.T.; Sørland, G.; Sjöblom, J. *J. Basic Princ. Diffus. Theory, Exp. Appl.* **2009**, 9, 1.

8. Peixinho, J.;Karanjkar, P.U.; Lee, J.W.; Morris, J.F. *Langmuir.* **2010**, 26 (14), 11699. doi: 10.1021/la101141j

9. Sjöblom, J; Øvrevoll, B; Jentoft, G; Lesaint, C; Palermo,T; … Koh, C.A. *J. Dispers. Sci. Tech*. **2010**, 31 (8), 1100. doi: 10.1080/01932690903224698.

10. Dunn, K.J.; Bergman, D.J.; Latorraca, G.A; *Nuclear Magnetic Resonance Petrophysical and Logging Applications*, Pergamon, **2002**.

11. Coates, G.R.; Xiao, L.; Prammer, M.G. *NMR Logging Principles & Applications,* Halliburton Energy Services Publication **1999**.

12. Lawson, C.L.; Hanson, R.J. *Solving Least Squares Problems. Series in Automatic Computation*, Prentice Hall. **1974**.

13. Hürlimann, M.D.; Venkataramanan, L.; Flaum, C.; Speier, P.; Karmonik, C.; … Heaton, N. *Diffusion-Editing: New NMR Measurement of Saturation and Pore Geometry*, SPWLA 43rd Annu. Logging Symp., **2002**.

14. Song, Y.Q; *Vadose Zone. J*. **2010**, 9, 828. doi:10.2136/vzj2009.0171.

15. Venkataramanan, L.; Song, Y.; Hürlimann, M.D. *IEEE Trans. Signal Process.* **2002**, 50 (5), 1017. doi: 10.1109/78.995059.

16. Dunn, K.; LaTorraca, G; Warner, J.L.; Bergman, D.J. *SPE Annu. Tech. Conference*, **1994**.

17. Packer, K, Rees, C. *J. Colloid Interface Sci.* **1972**, 40 (2), 206. doi:10.1016/0021-9797(72)90010-0.

18. Hirasaki, G.J.; Pena, A.A. *Advances Colloid Interface Sci.* **2003**, 105 (1-3), 103. doi:10.1016/S0001-8686(03)00092-7.

19. Johns, M.L. *Curr. Opin. Colloid Interface Sci.* **2009,** 14 (3), 178. doi:10.1016/j.cocis.2008.10.005.

20. Fridjonsson, E.O.; Graham, B.F.; Akhfash, M.; May, E.F; Johns, M.L. *Energy and Fuels*. **2014**, 28 (3), 1756. doi: 10.1021/ef402117k.

21. Sørland, G.H.; Keleşoğlu, S.; Simon, S. *J. Basic Princ. Diffus. Theory, Exp. Appl.* **2013**, 19, 1.

22. Lingwood, I.A.; Chandrasekera, T.C.; Kolz, J. ; Fridjonsson, E.O.; Johns, M.L. *J. Magn. Reson.* **2012,** 214 (1), 281. doi: 10.1016/j.jmr.2011.11.020.

23. Zhang, Y.; Hirasaki, G.; House, W.V. ; Kobayashi, R. *SPE J.* **2002**, **7**,1.

24. Murday, J.S.; Cotts, R.; *J. Chem. Phys.* **1968**, 48 (11), 4938. doi: 10.1063/1.1668160.

25. Noïk, C.; Trapy, J.; Mouret, A. *Soc. Petroelum Eng.* **2002**. doi: 10.2118/77492-MS